Pulse amplification in semiconductor optical amplifiers with ultrafast gain-recovery times

Prashant P. Baveja[a], Aaron M. Kaplan[a], Drew N. Maywar[b], and Govind P. Agrawal[a]

[a]Institute of Optics, University of Rochester, Rochester, NY, 14627 USA
[b]Deptt. of Telecommunication Engineering Technology, Rochester Institute of Technology, Rochester, NY 14623 USA

ABSTRACT

This paper presents detailed numerical and experimental study of SPM in semiconductor optical amplifiers (SOAs) with ultrafast gain-recovery times. These SOAs have a range of gain-recovery speed which is a function of drive current. At increased drive current, the amount of internal ASE in the SOA increases, which causes the small signal gain to saturate and reduces the gain-recovery time. Understanding pulse amplification in these SOAs is important for optimizing the performance of SOA-based optical regenerators and wavelength converters. Our study addresses the full range of gain-recovery times in commercial SOAs extending from less than 10 ps to >100 ps.

Keywords: gain recovery, amplified spontaneous emission (ASE), semiconductor optical amplifier (SOA), self-phase modulation (SPM), all optical signal processing.

1. INTRODUCTION

In future high-speed telecommunication systems, all-optical signal processing techniques promise to play a prominent role to avoid electro-optic conversions that may create data-flow bottlenecks. Semiconductor optical amplifiers (SOAs) have been widely used to perform a variety of all-optical functions such as wavelength conversion,[1] signal regeneration,[2] pulse reshaping,[3] and power limiting.[4] Compared to their fiber-based counterparts,[5–8] SOA based all-optical signal processing techniques have advantages in terms of low-power consumption, a small footprint, and monolithic integration.[9] However such techniques also have one serious limitation. While the nonlinear response of an optical fiber is almost instantaneous,[10] the nonlinear response time of a SOA is tied to its carrier lifetime[11] that governs how quickly the SOA gain recovers and typically exceeds 0.1 ns.

A lot of techniques have been used in the literature to reduce the gain-recovery time of SOAs.[13–23] These techniques can be grouped into three categories. The first category involves the use of SOAs made with semiconductor quantum dots[13–15] or doped quantum wells.[16] The second category involves using a CW beam, called the holding beam, that saturates the SOA because its wavelength lies within the SOA gain spectrum or near the transparency point.[17–19] The third category employs the amplified spontaneous emission (ASE) within the SOA to saturate it and to reduce its gain-recovery time.[20–23] Such *commerical* SOAs have ultrafast gain-recovery time as short as 10 ps. They are optimized carefully so that they can be driven at high drive currents (up to 500 mA in our case), and short gain-recovery times are realized only at high operating currents.[24] Although the nonlinear effects have been investigated in SOAs employing a holding beam for faster gain recovery,[25–27] to the best of our knowledge, no study has yet addressed the nonlinear effects in commercial ultrafast SOAs that achieve gain-recovery reduction using internal ASE.

In this paper we address a fundamental nonlinear effect, known as self-phase modulation (SPM), that leads to spectral broadening of optical pulses. This phenomenon in SOAs was first studied[11] in 1989. The physical mechanism behind SPM in SOAs was found to be gain saturation, which leads to intensity-dependent changes in the refractive index in response to variations in carrier density. In this work, however, gain-recovery time, limited by the carrier lifetime, was taken to be much longer than typical pulse widths employed in the experiment.[11]

The objective of this paper is to perform a comprehensive investigation into the spectral impact of pulse-amplification in semiconductor optical amplifiers with ultrafast gain-recovery times. In section 2 we extend the theoretical framework of Ref.[11] to include the impact of ASE-reduced gain-recovery and derive a simple expression for the amplification factor

Further author information: Send correspondence to Prashant P. Baveja E-mail: baveja@optics.rochester.edu

Optical Components and Materials VII, edited by Shibin Jiang, Michel J. F. Digonnet, John W. Glesener, J. Christopher Dries, Proc. of SPIE
Vol. 7598, 759817 · © 2010 SPIE · CCC code: 0277-786X/10/$18 · doi: 10.1117/12.841025

Downloaded from SPIE Digital Library on 06 Apr 2010 to 128.151.82.225. Terms of Use: http://spiedl.org/terms

in the continuous-wave (CW) case. In section 3, we present the CW experimental results and use them to extract a critical device parameter that governs the ASE level at a given current. We use this parameter to show how gain-recovery time is reduced at high drive currents. In section 4 we consider the amplification of picosecond pulses in ultrafast SOAs and study the impact of ASE-reduced gain-recovery on the SPM-induced nonlinear-phase shift and the corresponding frequency chirp imposed on the pulse. We study theoretically in section 5 the impact of ASE-reduced gain-recovery on the shape and spectrum of amplified pulses. We present in section 6 the experimental results on spectral impact of pulse-amplification. The main results of the paper are summarized in the last section.

2. THEORETICAL MODEL

The injection of current into an SOA creates electron and hole carriers, whose density N provides optical gain as $g = \Gamma a(N - N_0)$, where Γ is the mode confinement factor, a is a material parameter (referred to as the gain cross section), and N_0 is the value of carrier density at which the SOA becomes transparent. When an optical signal is launched into the SOA, its amplitude and phase change because of the gain provided by SOA and the associated changes in the refractive index. To describe this amplification process, we adopt the model developed by Agrawal and Olsson[11] and write the signal's electric field in the form:

$$\mathbf{E}(\mathbf{r}, t) = Re[\hat{x}F(x, y)A(z, t)e^{i(\beta_0 z - \omega_0 t)}], \tag{1}$$

where $\hat{x}$ is the polarization unit vector, $F(x, y)$ is the mode distribution, $A(z, t)$ is the complex amplitude of the signal, ω_0 is its carrier frequency, and $\beta_0 = \bar{n}\omega_0/c$ is the propagation constant of the optical mode with the effective index $\bar{n}$.

The signal amplitude evolves inside the SOA as,[11]

$$\frac{\partial A}{\partial z} + \frac{1}{v_g}\frac{\partial A}{\partial t} = \frac{g}{2}(1 - i\alpha)A, \tag{2}$$

where v_g is the group velocity and α is the linewidth enhancement factor responsible for changes in the mode index with changes in the carrier density that satisfies a rate equation of the form[12]

$$\frac{\partial N}{\partial t} = \frac{I}{qV} - \frac{N}{\tau_c} - \frac{g(N)}{\hbar\omega_0}|A|^2, \tag{3}$$

where V is the active volume and τ_c is the carrier lifetime. It is important to remember that τ_c itself depends on N. If we include both the radiative and nonradiative recombination processes, this dependence takes the form

$$\frac{1}{\tau_c} = (A_{nr} + B_{sp}N + C_a N^2), \tag{4}$$

where A_{nr} is the intrinsic nonradiative recombination rate, B_{sp} is the spontaneous recombination coefficient, and C_a represents the Auger recombination coefficient. The carrier-density rate equation can be used to obtain the following equation for the optical gain $g(z, t)$ itself:[11]

$$\frac{\partial g}{\partial t} = \frac{g_0 - g}{\tau_c} - \frac{g|A|^2}{E_{\text{sat}}}, \tag{5}$$

where $E_{\text{sat}} = \hbar\omega_0\sigma/a$ is the saturation energy and the unsaturated gain g_0 depends on the injected current I as

$$g_0(I) = \Gamma a N_0(I/I_0 - 1), \tag{6}$$

where $I_0 = qVN_0/\tau_{c0}$ is the current required for transparency and τ_{c0} is the carrier lifetime at $N = N_0$.

In ultrafast SOAs, ASE becomes large enough at high injection currents that it can itself saturate the SOA gain, and its effects should be incorporated within the preceding set of equations. A general theory should consider the amplification of spontaneous emission in both the forward and backward directions over the entire SOA gain bandwidth and the saturation of the SOA gain by the resulting ASE. Because of the stochastic nature of ASE, such a theory is quite complicated. Here, we adopt a simple approach by ignoring the noisy nature of the amplified signal and treat $A(z, t)$ as the average signal amplitude. However, we take into account the ASE induced gain-saturation by replacing $|A|^2$ in Eq. (5) with $|A|^2 + P_{\text{ASE}}$, where $P_{\text{ASE}} = P_f + P_b$ represents the sum of ASE powers in the forward and backward directions. Even though P_f and

Downloaded from SPIE Digital Library on 06 Apr 2010 to 128.151.82.225. Terms of Use: http://spiedl.org/terms

P_b change considerably along the SOA length because of exponential amplification of spontaneous emission, their sum is relatively constant. We simplify the following analysis by treating $P_{\rm ASE}$ as a constant whose value depends only on the current I injected into the SOA.

Before considering amplification of optical pulses, we first focus on the continuous-wave (CW) case and assume that a CW signal with input power $P_{\rm in}$ is injected into the SOA. Using $A(z) = \sqrt{P}e^{i\phi}$ in Eq. (2), the signal power and phase satisfy

$$\frac{dP}{dz} = g(z)P, \qquad \frac{d\phi}{dz} = -\frac{\alpha}{2}g(z). \tag{7}$$

Setting the time derivative to zero in Eq. (5), the signal power $P(z)$ is found to depend on $P_{\rm ASE}$ as

$$\frac{dP}{dz} = \frac{g_0(I)P}{1 + (P + P_{\rm ASE})/P_{\rm sat}}, \tag{8}$$

where the saturation power $P_{\rm sat}$ is defined as:[11]

$$P_{\rm sat} = \frac{E_{\rm sat}}{\tau_c} = E_{\rm sat}(A_{nr} + B_{sp}N + C_aN^2). \tag{9}$$

The ASE power also depends on the carrier density N. Since electron-hole recombination is the source of ASE, we expect ASE to scale as N^2, where both electron and hole densities are proportional to N and assume[12]

$$P_{\rm ASE} = DN^2. \tag{10}$$

where D is a constant whose value depends on a number of SOA parameters. Since we do not have an explicit expression for D, we estimate its value using an experiment that measures amplification factor $G(I)$ of a low-power CW signal, as a function of device current, in the small-signal regime. Before we describe the experiment in section 3, we obtain an analytic expression for $G(I)$.

In the small-signal regime, we can replace $P + P_{\rm ASE}$ in Eq. (8) with $P_{\rm ASE}$ because the SOA gain is saturated only by $P_{\rm ASE}$. Equation (8) can then be integrated easily to obtain $G(I) = P_{\rm out}/P_{\rm in}$, where $P_{\rm out} = P(L)$ and L is the SOA length. The final result is given by

$$G(I) = \exp\left(\frac{g_0(I)L}{1 + P_{\rm ASE}/P_{\rm sat}}\right), \tag{11}$$

where both $P_{\rm ASE}(N)$ and $P_{\rm sat}(N)$ also depend on I because the carrier density N changes with I.

3. GAIN SATURATION AND RECOVERY IN ULTRAFAST SOAS

Our experiment employed an ultrafast SOA designed to provide the gain-recovery time of 9 ps at the maximum drive current of 500 mA. Figure 1(a) shows the experimental setup used for measuring the small-signal gain of a weak CW signal as a function of drive current. The power of 1594.4-nm signal is limited to 2 μW to ensure that it does not saturate the amplifier. The power of amplified signal was measured after passing it through a 1-nm-bandwidth optical bandpass filter to reject the out-of-band portion of the ASE.

The symbols in Figure 1(b) show the measured values of $\ln G(I)$ as a function of drive current I. The coupling and other losses are included by adding 2 dB to the fiber-to-fiber gain values measured in the experiment.[28] It is evident from this figure that the CW signal is amplified exponentially (or linearly on the semi-log plot) for currents of up to 100 mA, but this exponential growth is reduced dramatically at higher currents because of gain saturation induced by the increasing ASE. The solid line shows a theoretical fit to the data based on the analytical expression in Eq. (11). The agreement between the theory and experiment in Fig. 1(b) is quite reasonable. We know $L = 1$ mm for our device. The dimensionless constant $\Gamma a N_0 L$ and transparency current I_0 in Eq. (6) are uniquely determined from the experimental data by using the gain values at low drive currents; they are found to be to be 7 and 30 mA respectively. Using the values of Γ and a from Table 1, we calculate $N_o = 1.6355 \times 10^{23} m^{-3}$. The volume of the device was calculated by substituting the values of N_o and I_o in Eq. (3). We calculated $V = 2.83 \times 10^{-16} m^3$ and consequently $E_{sat} = 0.843$ pJ.

Downloaded from SPIE Digital Library on 06 Apr 2010 to 128.151.82.225. Terms of Use: http://spiedl.org/terms

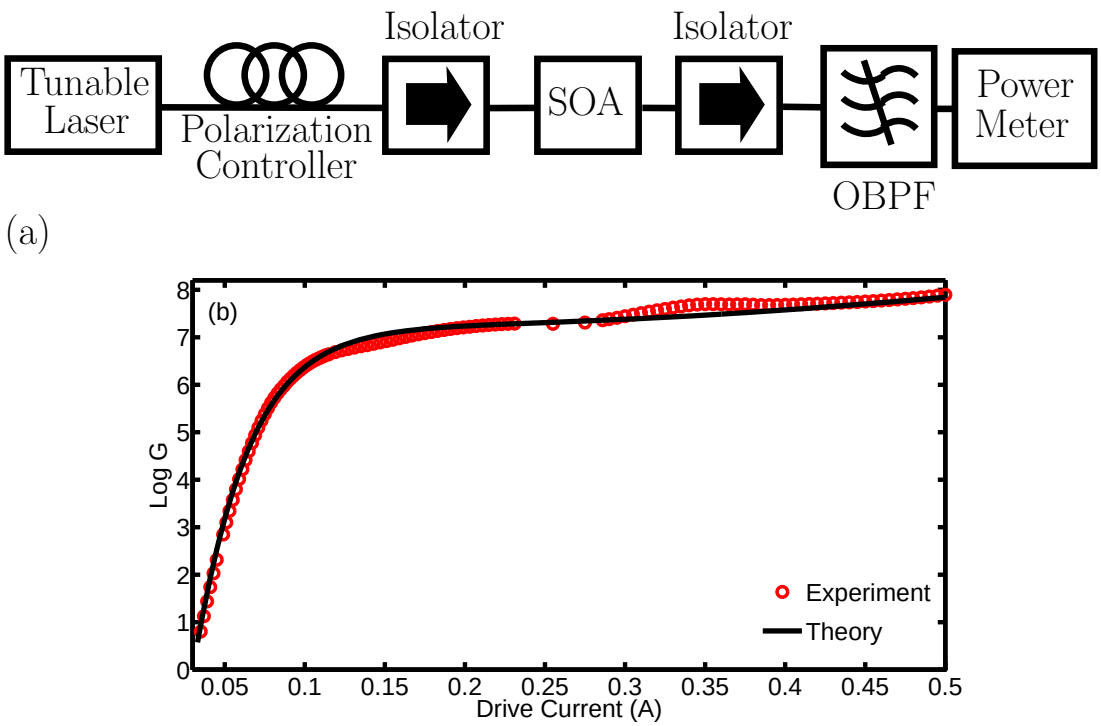

Figure 1. (a) Experimental setup and (b) log G as a function of drive current. The solid line corresponds to the best estimate of D from the experimental data (circles)..

Table 1. Assumed parameter values

Parameter	Our value	Typical values
Γ	0.4	0.3–0.7
a (m^2)	10.5×10^{-20}	2.5–4.5×10^{-20}
A_{nr} (s^{-1})	3.9×10^{9}	0.1–4.5×10^{9}
B_{sp} (m^3/s)	8.5×10^{-16}	1–9×10^{-16}
C_a (m^6/s)	3.3×10^{-40}	1–97×10^{-40}

To obtain the fit, we set the time derivative to zero in Eq. (3), neglect the last term, and solve for N at a given value of I by finding the real positive root of the cubic polynomial,

$$\frac{I}{qV} = \frac{N}{\tau_c} = N(A_{nr} + B_{sp}N + C_aN^2). \tag{12}$$

This allows us to calculate both $P_{\mathrm{ASE}}(N)$ and $P_{\mathrm{sat}}(N)$ as a function of I. The ASE parameter D in Eq. (10) was used as a fitting parameter and its value was found to be 2.32×10^{-50} m^{6}W for our device. Table 1 shows the values of other parameters used together with their typical values employed in the literature for different SOAs.[12,20,22,23,27,29–32] As seen there, the value of a is larger for our SOA. This is not surprising because ultrafast SOAs are designed for smaller values of E_{sat}.

We next use our model to study how the gain-recovery time is shortened at high drive currents by the increasing ASE. To see from where this current dependence originates, we include ASE in the gain equation Eq. (5) by replacing $|A|^2$ with $|A|^2 + P_{\mathrm{ASE}}$ and rewrite it in the form

Downloaded from SPIE Digital Library on 06 Apr 2010 to 128.151.82.225. Terms of Use: http://spiedl.org/terms

$$\frac{\partial g}{\partial t} = \frac{g_0}{\tau_c} - \frac{g}{\tau_{\text{eff}}} - \frac{g|A|^2}{E_{\text{sat}}}, \tag{13}$$

where the effective gain-recovery time is defined as

$$\frac{1}{\tau_{\text{eff}}} = \frac{1}{\tau_c} + \frac{1}{\tau_{\text{ASE}}} \tag{14}$$

and we have introduced a new ASE-related recombination time as

$$\frac{1}{\tau_{\text{ASE}}} = \frac{P_{\text{ASE}}}{E_{\text{sat}}} = D_{sp}N^2, \tag{15}$$

with $D_{sp} = D/E_{\text{sat}}$. Using equations (9), (14) and (15), τ_{eff} can be written in the form

$$\frac{1}{\tau_{\text{eff}}} = A_{nr} + B_{sp}N + (C_a + D_{sp})N^2. \tag{16}$$

This relation shows that the ASE contribution enters in the same fashion as the Auger contribution and can be included in practice by increasing the value of the Auger parameter C_a. Using the calculated value of E_{sat}, D_{sp} is found to be 2.75×10^{-38} m^6/s. If we compare this to the value of C_a in Table 1, we find that the ASE contribution to τ_{eff} for our SOA exceeds the Auger contribution by a factor of 83. Clearly, the presence of ASE shortens the gain-recovery time drastically. Figure 2 shows the calculated values of τ_{eff} as a function of drive current. At low drive currents below 50 mA, ASE contribution is negligible and our SOA has a gain-recovery time of 200 ps ($\tau_{\text{eff}} = \tau_c$). As current increases, ASE builds up and leads to a monotonic decrease in the value off τ_{eff}, resulting in a value of about 10 ps at $I = 0.5$ A. This behavior is in agreement with previous studies on this kind of SOAs[16,22] and also agrees with the quoted value of 9 ps at $I = 0.5$ A for our SOA.

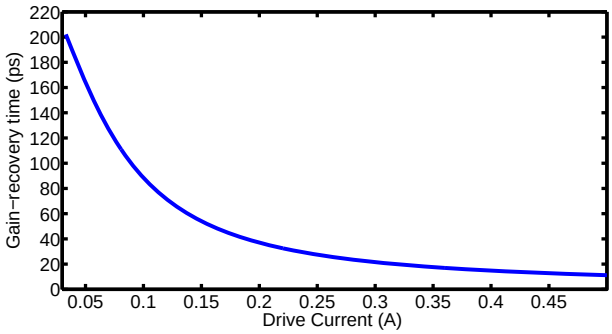

Figure 2. Calculated values of τ_{eff} as a function of drive current for the SOA used to obtain the data in Fig. 1.

4. SPM-INDUCED NONLINEAR PHASE SHIFT AND CHIRP IN ULTRAFAST SOAS

SPM or its variant, cross-phase modulation, is employed for many all-optical signal processing applications including wavelength conversion,[1] signal regeneration,[2] pulse compression,[33] channel multiplexing/demultiplexing,[34,35] and bit-level logic.[36] The nonlinear phase shift and the resulting chirp imposed on the pulse become important for any such SOA-based application.

In this section we study the SPM-induced nonlinear phase shift imposed on an optical pulse as it propagates through an ultrafast SOA. In the case of pulses, it is useful to rewrite the amplitude equation Eq. (2) in a frame moving with the pulse. Introducing the reduced time as $\tau = t - z/v_g$ together with $A = \sqrt{P}e^{i\phi}$ in Eq. (2), the signal power $P(z,\tau)$ and the phase $\phi(z,\tau)$ are found to satisfy

$$\frac{\partial P}{\partial z} = g(z,\tau)P, \qquad \frac{\partial \phi}{\partial z} = -\frac{\alpha}{2}g(z,\tau). \tag{17}$$

These equations look similar to their CW part in Eq. (7) except that all variables depend on the time τ implicitly. They can be integrated over the SOA length L to obtain

Downloaded from SPIE Digital Library on 06 Apr 2010 to 128.151.82.225. Terms of Use: http://spiedl.org/terms

$$P_{\text{out}}(\tau) = P_{\text{in}}(\tau)\exp[h(\tau)], \qquad \phi_n(\tau) = -\frac{\alpha}{2}h(\tau), \tag{18}$$

where $h(\tau) = \ln G(\tau) = \int_0^L g(z,\tau)$ represents the integrated gain at time τ, $P_{\text{in}}(\tau)$ represents the power profile of the input pulse, and the SPM-induced nonlinear phase shift is defined as $\phi_n(\tau) = \phi(L,\tau) - \phi(0,\tau)$. We can obtain an equation for $h(\tau)$ by integrating the gain equation Eq. (13) over the SOA length.[11] The result is given by

$$\frac{dh}{d\tau} = \frac{g_0 L}{\tau_c} - \frac{h}{\tau_{eff}} - \frac{P_{in}(\tau)}{E_{\text{sat}}}(e^h - 1). \tag{19}$$

Once this equation is integrated numerically, both the power and phase profiles of the amplified pulse can be obtained.

The frequency chirp $\Delta\nu_0$ imposed on the pulse is related to the nonlinear phase as $2\pi\Delta\nu_0 = -d\phi_n/d\tau$.[11] Using $\phi_n(\tau)$ from Eq. (18), the chirp is given by

$$\Delta\nu_0(\tau) = \frac{\alpha}{4\pi}\frac{dh}{d\tau}, \tag{20}$$

where $dh/d\tau$ is obtained from (19).

To illustrate the nonlinear phase and the frequency chirp at the output of an ultrafast SOA, we consider a 20-ps full-width at half maximum (FWHM) Gaussian input pulse with the power profile $P(t) = P_0\exp(-t^2/\tau_p^2)$. When (FWHM) is 20 ps, the parameter $\tau_p \approx 12$ ps. We assume that the input pulse energy corresponds to $E_{in}/E_{\text{sat}} = 0.3$. The linewidth enhancement factor, α, is taken to be 5. The SOA is operated at a current of 0.5 A at which the small-signal CW amplification factor corresponds to $G = e^{7.8} = 33.9$ dB in Fig. 1. The solid curves in Figure 3 show the temporal profiles for the nonlinear phase shift $\phi_n(\tau)$ and for the chirp $\Delta\nu_0(\tau)$ using $\tau_{\text{eff}} = 10$ ps, the value we deduced in Section III. For comparison, the dashed lines show the case of a standard SOA with same amplification factor and α-factor as the ultrafast SOA and using $\tau_{eff} = 200$ ps. Clearly, the SPM process is very different for ultrafast SOA as opposed to a standard SOA, both qualitatively and quantitatively.

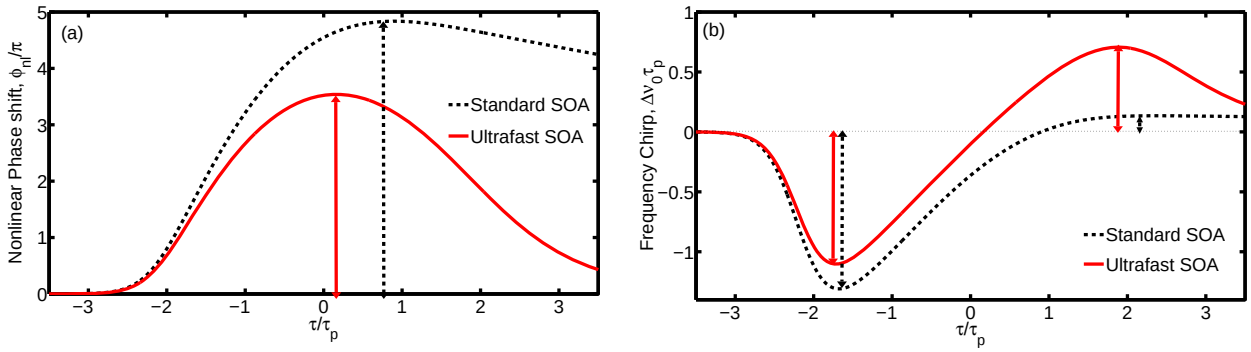

Figure 3. (a) Nonlinear Phase and (b) frequency chirp induced on a 20-ps-wide Gaussian pulse by an ultrafast SOA. Dashed lines show the case for standard SOA. The double arrows indicate the maximum value of nonlinear phase and chirp for both the cases.

For a standard SOA, our theory reduces to the case when the pulse width is a small fraction of the gain-recovery time of 200 ps.[11] The nonlinear phase shows a rapid increase as the leading edge of the pulse saturates the SOA gain, and a reduction in the carrier density increases the mode index. Since the gain cannot recover much over the pulse duration, the nonlinear phase saturates with only slight reduction in the trailing part of the pulse. The situation changes considerably for the ultrafast SOA at the maximum drive current. Now, the saturated gain can recover within the pulse duration. As a result, the carrier density begins to increase in the trailing region of the pulse. The resulting decrease in the mode index then leads to a rapid reduction in the pulse phase as well. The net result is the the phase profile becomes much more symmetric and begins to mimic the shape of the amplified pulse. This is precisely what occurs in the case of optical fibers whose nonlinearity responds on a femtosecond time scale.[10] The fiber-like features of SPM in ultrafast SOAs are potentially attractive for designing SOA based devices such as all-optical regenerators and switches. The nonlinear phase shifts can also be used in an interferometric configuration for all-optical signal-processing applications.[37]

Downloaded from SPIE Digital Library on 06 Apr 2010 to 128.151.82.225. Terms of Use: http://spiedl.org/terms

The chirp profiles in Figure 3(b) shows how the gain-dynamics in an ultrafast SOA affect the frequency chirp imposed by the SPM on an amplifying pulse. In the presence of ASE, the extent of red chirp is reduced slightly but there is a significant increase in blue chirp due to ASE-induced faster gain recovery. The net result is an almost linear chirp across the center part of the pulse, a behavior similar to that occurring in optical fibers.[10] This linear chirp is very attractive for compressing the amplified pulse.[38] It is worth noting that the required peak power of pulses is smaller by a factor of 1000 or more when ultrafast SOAs are used[11] compared with optical fibers that typically require a few watts of peak power in practice. The main point to note is that the ASE changes the gain dynamics of ultrafast SOAs in such a way that the SPM features begin to resemble those found in optical fibers, but they occur at peak-power levels that are orders of magnitude lower than those required for optical fibers.

5. PULSE SHAPES AND SPECTRA

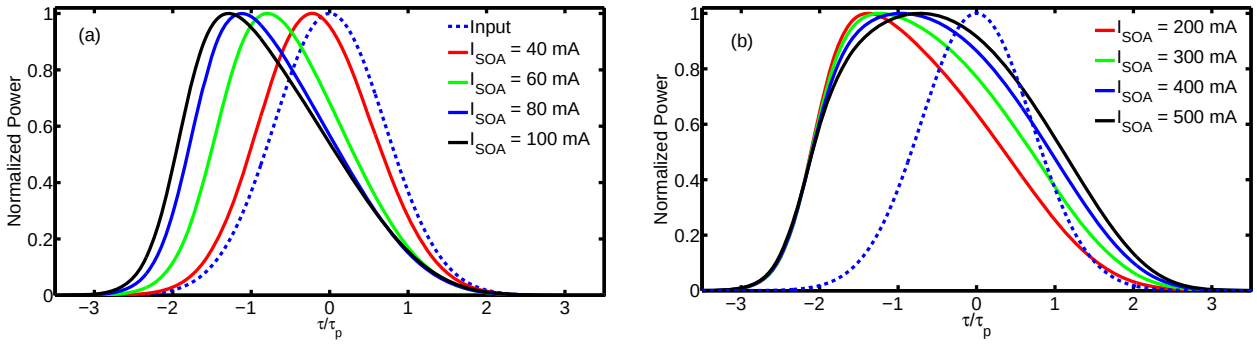

Figure 4. Output pulse shapes (a) at relatively low drive currents of up to 100 mA and (b) at drive currents of 200, 300, 400, 500 mA.

Changes in the frequency chirp due to ASE induced gain-dynamics also affect the spectrum of the amplified pulse. In this section we look at the shape and the spectrum of the output pulse when a 20-ps Gaussian input pulse is amplified by the SOA at different drive currents. The pulse shape is obtained from Eq. (18), and the results are shown in Fig. 4. All parameters were identical to those used in Section IV.

At low drive currents, ASE power is negligible, and the gain-recovery time is much longer than the pulse width.[11] As shown in Fig. 4(a), the amplified pulse acquires an asymmetric shape with a leading edge sharper than the trailing edge. This is attributed to the fact that the leading edge of the pulse experiences full gain, but the gain is reduced substantially for the trailing edge, because the amplification of pulse's leading part saturates the SOA gain. At low drive currents, the ultrafast SOA thus behaves like a standard SOA. However at drive currents above 100 mA, the increasing ASE itself begins to saturate the gain and to reduce the gain-recovery time to below 100 ps, making it comparable to the pulse width. As seen in Fig. 4(b), the trailing edge of the pulse becomes progressively sharper as drive current increases, with no visible change near the leading edge of the pulse. Physically, this can be understood by recalling that a faster gain recovery allows the gain to recover so quickly that the training edge begins to experience a much higher gain. The important feature to note is that the pulse shape becomes much more symmetric, although it deviates considerably from the input pulse shape.

The pulse spectrum is obtained by taking the Fourier transform of the output field $A(L,\tau)$, and the results are shown in Fig. 5 for drive currents ranging from 40 to 500 mA. At low drive currents of up to 100 mA, the output spectrum is highly asymmetric, with most of pulse energy contained in two red-shifted spectral lobes. This kind of spectrum is associated with standard SOAs.[11] At high drive currents seen in Fig. 5(b), energy is transferred from the red to blue side of the pulse spectrum, and the blue-shifted spectral lobes increase in amplitude progressively. These changes in the pulse spectra can again be understood in terms of the faster gain recovery induced by the increasing ASE. At low drive currents, the gain-recovery time is longer than the pulse width, and the trailing part of the pulse does not experience much blue chirp (see Fig. 3), resulting in an asymmetric red-shifted pulse spectrum. As long as the contribution of ASE is negligible, the spectral asymmetry increases with increasing drive current. At drive currents of 200 mA or more, ASE power becomes large enough that the gain-recovery time is reduced considerably. This enhanced gain recovery imposes a blue chirp on the trailing part of the pulse and increases the spectral symmetry in the output spectrum. This situation is similar to that occurring for optical fibers in which SPM is due to the quasi-instantaneous Kerr-type nonlinearity, resulting in a totally symmetric spectrum.[10]

Downloaded from SPIE Digital Library on 06 Apr 2010 to 128.151.82.225. Terms of Use: http://spiedl.org/terms

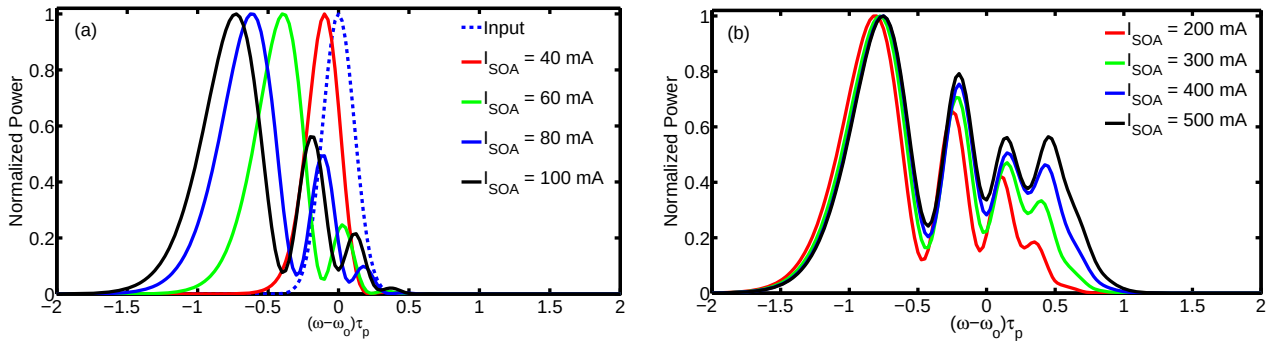

Figure 5. Output pulse spectrum (a) at relatively low drive currents of up to 100 mA and (b) at drive currents of 200, 300, 400, 500 mA with increasing ASE contribution.

6. EXPERIMENTAL RESULTS

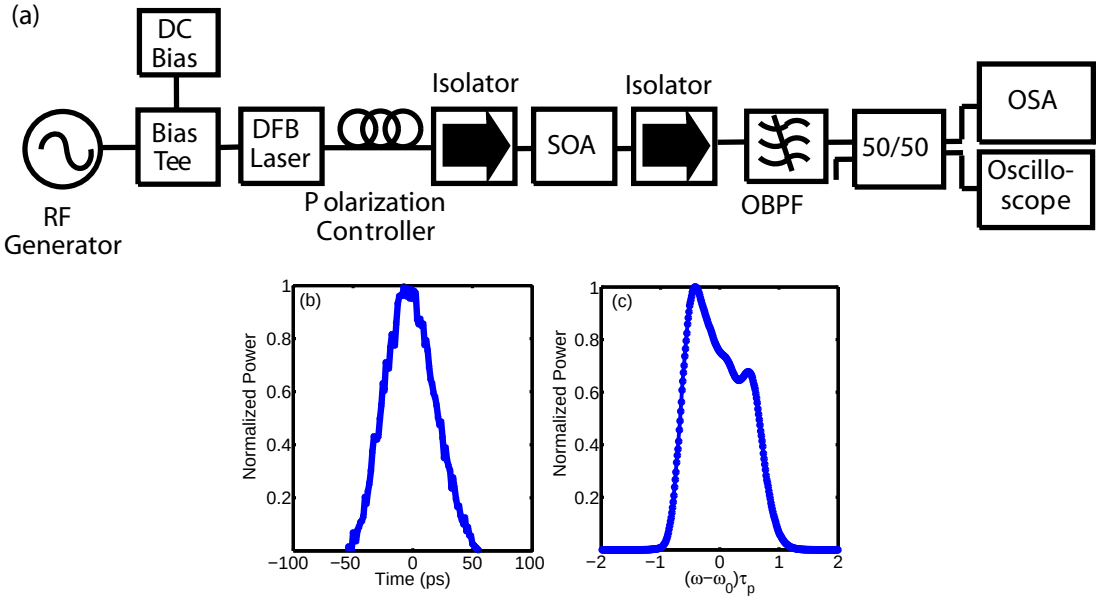

Figure 6. (a) Experimental setup. (b) Pulse shape and (c) pulse spectrum produced by the gain-switched DFB laser.

To verify the theory developed in this paper, we have measured pulse spectra for the same ultrafast SOA whose measured gain under CW conditions is shown in Fig. 1. The experimental setup of Fig. 6(a) was employed for this purpose. We use gain switching[39,40] of a multiquantum-well distributed feedback (DFB) laser to produce optical pulses with a full width at half-maximum of 57 ps at a wavelength of 1594.41 nm. The DFB laser module is part of an ILX lightwave mount whose bias-T circuitry accepts radio-frequency (RF) signals up to 2.5 GHz. The threshold current of the laser was 25 mA at 25°C. To obtain gain-switched pulses, the laser was biased at 14.89 mA and driven with a 1-GHz RF signal with 64.4 mA peak amplitude. Figure 6 shows (b) the shape and (c) the spectrum of the resulting gain-switched pulses. The central frequency $\nu_0 = 188.23$ THz is defined using the first moment of the spectrum. The pulse shape is gaussian with 57 ps FWHM. This corresponds to $\tau_p = 34.2$ ps. The peak power of our gain-switched pulses was 3 mW. We estimate the chirp parameter[10] to be $C = -4.91$. The observed spectrum is asymmetric due to this negative chirp imposed on the pulse during the gain-switching process. On the diagnostic end of the experimental setup, an optical bandpass filter with a 3-dB bandwidth of 1 nm was used to reject the out-of-band portion of ASE noise. A 50/50 splitter was employed to send the amplified pulses simultaneously into an optical spectrum analyzer (resolution 0.01 nm) and a photodiode with 22-GHz bandwidth. The oscilloscope was a 70 GHz sampling scope with 1.25 ps resolution.

Figure 7 shows the measured optical spectra of amplified pulses at the SOA output as the drive current is varied from

Downloaded from SPIE Digital Library on 06 Apr 2010 to 128.151.82.225. Terms of Use: http://spiedl.org/terms

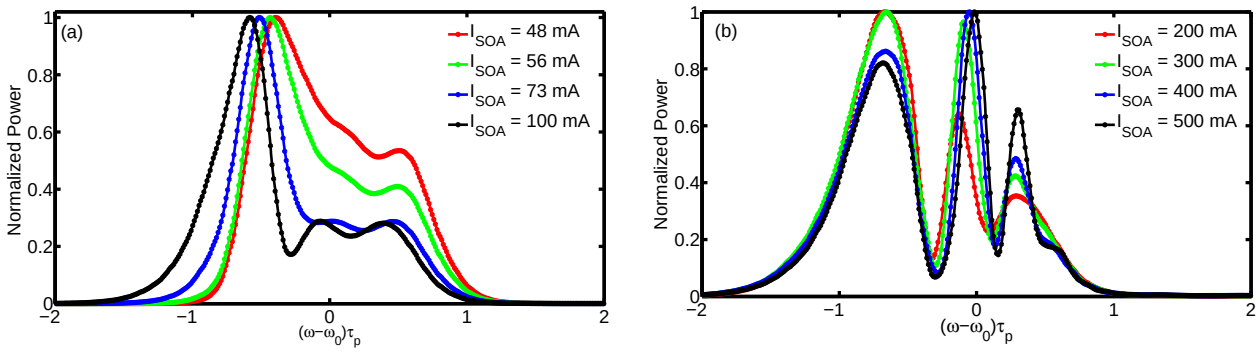

Figure 7. Observed spectra of amplified pulses at drive current (a) up to 100 mA and (b) beyond 100 mA.

40 to 500 mA. For the relatively low drive currents shown in Fig. 7(a), as the drive current is increased, the energy in the red-shifted spectral lobe increases at the expense of much reduced relative energy in the blue-shifted spectral region. However, the SOA shows a dramatically different behavior for currents beyond 100 mA, as evident from Fig. 7(b). The relative energy of the red-shifted spectral lobe decreases, and at the same time the relative energies in the central lobe and the blue-shifted spectral lobe increase. As a result of these changes, the output spectrum progressively becomes more symmetric. the experimental observation agree well with the theoretical calculations shown in Figure 5

7. DISCUSSIONS AND CONCLUSIONS

This paper has studied, both theoretically and experimentally, pulse amplification in ultrafast SOAs. We used the small-signal CW gain measurements and a detailed theoretical model to deduce how ASE shortens the effective gain-recovery time, τ_{eff}, of these SOAs to values near 10 ps. We incorporated the current dependence of τ_{eff} and the SOA gain into a simple numerical model and studied the amplification of picosecond pulses inside ultrafast SOAs which achieve accelerated gain-recovery at high drive currents due to internal ASE.

Our results show that the amplification process in ultrafast SOAs is different in several ways. The SPM-induced nonlinear phase shift becomes much more symmetric and, consequently, frequency chirp becomes much more linear across the pulse, a feature that is attractive for designing SOA-based all-optical signal-processing devices such as wavelength converters, regenerators and switches. The trade-off between the maximum nonlinear phase-shift and nonlinear-phase recovery is governed by the ratio of pulse width to τ_{eff}. Since τ_{eff} can be controlled by changing the drive current, a single SOA can potentially be optimized for different input pulse widths.

We calculated the shape and spectrum of amplified pulses over a range of drive currents to study how they change with shortening of the gain-recovery time. The pulse shape becomes much more symmetric at high drive currents because a reduction in the value of τ_{eff} causes the gain to recover fast enough that both the leading and trailing edge of the pulse experiencing nearly the same gain. For the same reason, the output spectrum becomes more symmetric and resembles that obtained in the case in optical fibers where SPM occurs due to a nearly instantaneous Kerr nonlinearity. We verified our theoretical predictions with an experiment in which we measured pulse spectra using gain-switched input pulses. Our experimental results agree well with the theoretical predictions. The main point to note is that the ASE influences the gain dynamics in ultrafast SOAs in such a way that the SPM features begin to resemble those found in optical fibers, but they occur at peak-power levels that are orders of magnitude lower than those required for optical fibers.

Acknowledgments

This work is supported in part by the NSF award ECCS-0822451. The support of NSF does not constitute an endorsement of the views expressed in this article.

REFERENCES

1. J. Leuthold, R. Ryf, D. N. Maywar, S. Cabot, J. Jacques, and S. S. Patel, "Nonblocking all-optical cross connect based on regenerative all-optical wavelength converter in a transparent demonstration over 42 nodes and 16,800 km," *J. Lightwave. Technol.*, vol. 21, no. 1, pp. 2863–2870, Nov. 2003.

Downloaded from SPIE Digital Library on 06 Apr 2010 to 128.151.82.225. Terms of Use: http://spiedl.org/terms

2. M. P. Dlubek, A. J. Phillips, and E. C. Larkins, "Extinction ratio improvement using nonlinear four-wave mixing in SOAs with assist beam," *Microwave Opt. Technol. Lett.*, vol. 50, no. 8, pp. 2079–2083, Aug. 2008.
3. G. Contestabile, M. Presi, and R. Proiletti, and E. Ciaramella, "Optical reshaping of 40-Gb/s NRZ and RZ signals without wavelength conversion," *IEEE Photon. Technol. Lett.*, vol. 20, no. 15, pp. 1133–1135, July 2008.
4. G. Contestabile, M. Presi, R. Proiletti, N. Calabretta, and E. Ciaramella, "A simple and low-power optical limiter for multi-GHz pulse trains," *Opt. Express*, vol. 15, no. 15, pp. 9849–9858, July 2007.
5. P. V. Mamyshev, "All-optical regeneration based on self-phase modulation effect," in *Proc. Eur. Conf. Optical Communication (ECOC98)*, Madrid, Spain, Sep. 20-24, 1998, pp. 475–476.
6. E. Ciaramella, and S. Trillo, "All-optical signal reshaping via four-wave mixing in optical fibers," *IEEE Photon. Technol. Lett.*, vol. 12, no. 7, pp. 849–851, July 2000.
7. A. Bogoni, P. Ghelfi, M. Scaffardi, and L. Poti, "All-Optical Regeneration and Demultiplexing for 160-Gb/s Transmission Systems Using a NOLM-Based Three-Stage Scheme," *IEEE J. Sel. Top. Quantum Electron.*, vol. 10 no. 1, pp. 192–196, Jan. 2004.
8. S. Radic, C. J. McKinstrie, R. M. Jopson, J. C. Centanni, and A. R. Chraplyvy, "All-Optical Regeneration in One- and Two-Pump Parametric Amplifiers Using Highly Nonlinear Optical Fiber," *IEEE Photon. Technol. Lett.*, vol. 15, no. 7, pp. 957–959, July 2003.
9. T. Houbavlis, K. E. Zoiros, M. Kalyvas, G. Theophilopoulos, C. Bintjas, K. Yiannopoulos, N. Pleros, K. Vlachos, H. Avramopoulos, L. Schares, L. Occhi, G. Guekos, J. R. Taylor, S. Hansmann, and W. Miller, "All optical signal processing and applications within the Esprit project DO-ALL," *IEEE J. Lightwave. Technol.*, vol. 23, no. 2, pp. 781–801, Feb. 2005.
10. G. P. Agrawal, *Nonlinear Fiber Optics*, 4th ed., Academic Press, Boston, 2007.
11. G. P. Agrawal and N. A. Olsson, "Self phase modulation and spectral broadening of optical pulses in semiconductor laser amplifiers," *IEEE J. Quantum Electron.*, vol. 25, no. 11, pp. 2297–2306, Nov. 1989.
12. G. P. Agrwal and N. K. Dutta, *Semiconductor Lasers*, 2nd ed., Van Nostrand Rienhold, New York (1993)
13. M. Sugawara, N. Hatori, M. Ishida, H. Ebe, Y. Arakawa, T. Akiyama, K. Otsubo, T. Yamamoto and Y. Nakata, "Recent progress in self-assembled quantum-dot optical devices for optical telecommunication: temperature insensitive 10 Gb/s directly modulated lasers and 40 Gb/s signal regenerative amplifiers," *J. Phys. D: Appl. Phys.*, vol. 38, no. 13, pp. 2126–2134, Jul. 2005.
14. A. J. Zilkie, J. Meier, P. W. E. Smith, M. Mojahedi, J. S. Aitchison, P. J. Poole, C. N. Allen, P. Barrios, and D. Poitras, "Femtosecond gain and index dynamics in an InAs/InGaAsP quantum dot amplifier operating at 1.55 μm," *Opt. Express*, vol. 14, no. 23, pp. 11453–11459, Nov. 2006.
15. S. Dommers, V. V. Temnov, U. Woggon, J. Gomis Brescó, J. Martnez Pastor, M. Laemmlin, and D. Bimberg, "Gain Dynamics after Ultrashort Pulse Trains in Quantum Dot Based Semiconductor Optical Amplifiers," in *Conference on Lasers and Electro-Optics*, Baltimore, Maryland, May 6, 2007, paper CMM4.
16. L. Zhang, I. Kang , A. Bhardwaj, N. Sauer, S. Cabot, J. Jaques, and D. T. Nielson, "Reduced recovery time semiconductor optical amplifiers using p-type-doped multiple quantum wells," *IEEE Photon. Technol. Lett.*, vol. 18, no. 22, pp. 2323–2325, Nov. 2006.
17. M. A. Dupertuis, J. L. Pleumeekers, T. P. Hessler, P. E. Selbmann, B. Deveaud, B. Dagens, and J. Y. Emery, "Extremely fast high-gain and low-current SOA by optical speed-up at transparency," *IEEE Photon. Technol. Lett.*, vol. 12, no. 11, pp. 1453-1455, Nov. 2000.
18. J. Pleumeekers, M. Kauer, K. Dreyer, C. Burrus, A. G. Dentai, S. Shunk, J. Leuthold, and C. H. Joyner, "Acceleration of gain recovery in semiconductor optical amplifiers by optical injection near transparency wavelength," *IEEE Photon. Technol. Lett.*, vol. 14, no. 1, pp. 12–14 Jan. 2002.
19. G. Talli and M. J. Adams, "Gain recovery acceleration in semiconductor optical amplifiers employing a holding beam," *Opt. Commun.*, vol. 245, no. 1-6, pp. 363–370, Jan. 2005.
20. F. Girardin, G. Guekos, and A. Houbavlis, "Gain recovery of bulk semiconductor optical amplifiers," *IEEE Photon. Technol. Lett.*, vol. 10, no. 6, pp. 784–786, Jun. 1998.
21. F. Ginovart and J.C. Simon, "Gain dynamics studies of a semiconductor optical amplifier," *J. Opt. A-Pure Appl. Opt.*, vol. 4, no. 3, pp. 283–287, May 2002.
22. R. Giller, R.J. Manning, G. Talli, R. P. Webb, and M. J. Adams, "Analysis of the dimensional dependence of semiconductor optical amplifier recovery speeds," *Opt. Exp.*, vol. 15, no. 4, pp. 1773–1782, Feb. 2007.

Downloaded from SPIE Digital Library on 06 Apr 2010 to 128.151.82.225. Terms of Use: http://spiedl.org/terms

23. A. M. de Melo, and K. Petermann, "On the amplified emission noise modelling of semiconductor optical amplifiers," *Opt. Commun.*, vol. 281, no. 18, pp. 4598–4605, Sept. 2008.
24. A. Borghesani, "Semiconductor optical amplifiers for advanced optical applications," *Proc. 8th Int. Conf. Transparent Opt. Netw. (ICTON 2006)*, Nottingham, U.K., Jun. 18-22, 2006, pp. 119–122.
25. P. M. Gong, J. T. Hsieh, S. L. Lee, and J. Wu, "Theoretical analysis of wavelength conversion based on four-wave-mixing in light-holding SOA's," *IEEE J. Quantum Electron.*, vol. 40, no. 1, pp. 31–40, Jan. 2004.
26. R. Inohara, K. Nishimura, M. Tsurusawa, and M. Usami, "Experimental analysis of cross-phase modulation and cross-gain modulation in SOA injecting CW assist light," *IEEE Photon. Technol. Lett.*, vol. 15, no. 9 pp. 1192–1194, Sep. 2003.
27. H. Wang, J. Wu, J. Lin, "Spectral characteristics of optical pulse amplification in SOA under assist light injection," *J. Lightwave Technol.*, vol. 23, no. 9, pp. 2761–2771, Sep. 2005.
28. A. Borghesani, N. Fensom, A. Scott, G. Crow, L. Johnston, J. King, L. Rivers, S. Cole, S. Perrin, D. Scrase, G. Bonfrate, A. Ellis, I. Lealman, G. Crouzel, L. H. K. Chun, A. Lupu, E. Mahe, and P. Maigne, "High saturation power (>16.5 dBm) and low noise figure (< 6 dB) semiconductor optical amplifier for C-band operation," in *Proc. OFC*, Atlanta, March 23-28, 2003, pp. 534–536
29. S. Bischoff, M. L. Nielsen, and J. Mørk, "Improving the all-optical response of SOAs using a modulated holding signal," *J. Lightwave. Technol.*, vol. 22, no. 5, pp. 1303–1308 May 2004.
30. P. Morel and A Sharaiha, "Wideband time-domain transfer matrix model equivalent circuit for short pulse propagation in semiconductor optical amplifiers," *IEEE J. Quantum Electron.*, vol. 45, no. 2, pp. 103–114, Feb. 2009.
31. G. Giuliani and D. D. Alessandro, "Noise analysis of conventional and gain-clamped semiconductor optical amplifiers," *J. Lightwave. Technol.*, vol. 18, no. 9, pp. 1256–1263 Sept. 2000.
32. D. A. Reid, A. M. Clarke, X. Yang, R. Maher, R. P. Webb, R. J. Manning, and L. P. Barry, "Characterization of a turbo-switch SOA wavelength converter using spectrographic pulse measurement," *IEEE J. Sel. Topics Quantum Electron.*, vol. 14, no. 3, pp. 841–848, May/Jun. 2008.
33. N. A. Olssson, G. P. Agrawal, and K. W. Wecht, "16 Gbit/s, 70 km pulse transmission by simultaneous dispersion and loss compensation with 1.5 um optical amplifiers," *Electron. Lett.*, vol. 25, no. 9, pp. 603–605, Apr. 1989.
34. J. P. Sokoloff, P. R. Prucnal, I. Glesk, and M. Kane, "A terahertz optical asymmetric demultiplexer (TOAD)," *IEEE Photon. Technol. Lett*, vol. 5, no. 7, pp. 787–790, Jul. 1993.
35. C. Schubert, C. Schmidt, S. Ferber, R. Ludwig, and H. G. Weber, "Error-free all-optical add-drop multiplexing at 160 Gbit/s," *Electron. Lett.*, vol. 39, no. 14, pp. 1074–1075, Jul. 2003.
36. J. Dong , X. Zhang , S. Fu , J. Xu , P. Shum, and D. Huang, "Ultrafast all-optical signal processing based on single semiconductor optical amplifier and optical filtering," *IEEE J. Sel. Topics Quantum Electron.*, vol. 14, no. 3, pp. 770–778, May/Jun. 2008.
37. Y. Ueno, S. Nakamura, and K. Tajima, "Nonlinear phase shifts induced by semiconductor optical amplifiers with control pulses at repetition frequencies in the 40-160-GHz range for use in ultrahigh-speed all-optical signal processing," *J. Opt. Soc. Am. B*, vol. 19, no. 11, pp. 2573–2589, Nov. 2002.
38. G. P. Agrawal, *Applications of Nonlinear Fiber Optics*. Boston: Academic, 2001.
39. K. Y. Lau, "Gain switching of semiconductor injection laser," *Appl. Phys. Lett.*, vol. 52, no. 4, pp. 257–259, Jan. 1988.
40. P. P. Vasil'ev, "Ultrashort pulse generation in diode laser," *Opt. Quantum Electron.*, vol. 24, no. 4 pp. 801–824, Aug. 1992.

Downloaded from SPIE Digital Library on 06 Apr 2010 to 128.151.82.225. Terms of Use: http://spiedl.org/terms